Acta Cryst. (1955). 8, 142

Fourier Transforms and Scattering Intensities of Tubular Objects

BY JÜRG WASER

Department of Chemistry, The Rice Institute, Houston, Texas, U.S.A.

(*Received* 4 *August* 1954)

Fourier transforms and scattering intensities of discrete circles, arcs, cylinders, and of tubes consisting of concentric cylinders, are derived and discussed. An expression resembling the structure factor of crystals is given. For all these cases the intensity function shows bands with sharp edges on the inside and long tails in a direction perpendicular to the Z axis (chosen parallel to the axis of the object). The locations in reciprocal space of the edges are determined by the geometry of the nets on which the cylinders are based, while the region close to the Z axis is characteristic mainly of the large-scale structure of the object. Finally, the scattering due to a continuously wound-up sheet, consisting of one or several layers of unit cells, is discussed.

Introduction

Electron-diffraction patterns of single specimens of tubular fragments of halloysites obtained by Taggart, Milligan & Studer (1954) make it desirable to develop the diffraction theory of such objects. These tubular fragments consist of one or more wound-up sheets, each of which is made up of one or more layers. The radii of the tubes are large compared to the linear dimensions of the 'unit cells' of the basic structure of the layers. It is not certain, however, how the sheets are wound up in detail. Each tube, for instance, may contain a set of concentric circular cylinders, each consisting of one continuous sheet. Another possibility is that each halloysite tube contains a number of turns of the same sheet, wound up in a spiral fashion. The electron-microscopic evidence of Taggart, Milligan & Studer (1954) favors this latter concept.

This paper represents a theoretical discussion of the Fourier transforms and scattering intensities of discrete tubular objects. The two-dimensional cases of a circular set of points and of a discrete circular arc are treated first. A discussion of the nature of the transforms, all of which contain Bessel functions of high orders, is given, as well as of the squares of their absolute values. It involves asymptotic expansions and averaging over the oscillatory nature of the Bessel functions. Next, the transform of the three-dimensional cylinder is obtained by adding the contributions of circles which are spaced evenly and in definite phase relation along an axis perpendicular to their planes. The scattering intensities of tubes consisting of concentric cylinders will be described in detail, and an expression analogous to the structure factor of crystals will be derived. The scattering characteristic of spiral cylinders which result from winding up a continuous sheet will be discussed in a semi-quantitative fashion only. Finally, a scattering photograph will be discussed.

Transforms of circles and circular arcs

Let N points be evenly spaced along the circumference of a circle of radius r. If the first point has polar coordinates $(r, \varphi_0 = \delta)$, then those of the general point j are $(r, \varphi_j = \delta + 2\pi j/N)$, while the cartesian coordinates have the values

$$x_j = r\cos\varphi_j,\ y_j = r\sin\varphi_j,\ j = 0, \ldots, (N-1)\,. \quad (1)$$

The Fourier transform $T_{\text{cir.}}$ of the above set of points is defined by

$$T_{\text{cir.}}(R, \Phi) = \sum_{j=0}^{N-1} \exp\left[2\pi i(x_j X + y_j Y)\right]\,. \quad (2)$$

It is conveniently transformed from the cartesian coordinates X, Y of Fourier space to polar coordinates R, Φ, defined by the equations

$$X = R\cos\Phi,\ Y = R\sin\Phi\,. \quad (3)$$

Thus, remembering the definition of the scalar product, we have

$$T_{\text{cir.}}(R, \Phi) = \sum_{j=0}^{N-1} \exp\left[2\pi i r R\cos(\Phi - \varphi_j)\right]\,. \quad (4)$$

To get rid of the cosines we replace the exponential functions in the sum by a series of Bessel functions J_p, employing the relation (Watson, 1944)

$$\exp(ix\cos\alpha) = \sum_{p=-\infty}^{\infty} i^p J_p(x)\exp(ip\alpha)\,. \quad (5)$$

After reversing the order of summation and inserting the values of φ_j, we have

$$T_{\text{cir.}}(R, \Phi) = \sum_{p=-\infty}^{\infty} i^p J_p(2\pi r R) \times \exp\left[ip(\Phi - \delta)\right] \sum_{j=0}^{N-1} \exp(-2\pi i p j/N)\,. \quad (6)$$

The last sum equals N when $p = nN$ and vanishes otherwise, so that finally

$$T_{\text{cir.}}(R, \Phi) = N \sum_{n=-\infty}^{\infty} J_{nN}(2\pi rR) \exp [inN(\Phi + \pi/2 - \delta)] . \tag{7}$$

Although this expression, involving Bessel functions of high order, appears to be quite complex, its actual nature is much simpler, owing to the character of these functions. While the term with $n = 0$ is the function J_0 which resembles a cosine with slowly decreasing amplitude, all other terms contain Bessel functions of the high order $nN(n = \pm 1, \pm 2, \ldots)$, N having a three- or possibly four-digit value. Each of these functions remains close to zero until its argument has come close to the value of its order. For still larger arguments the functions are of oscillatory nature, with slowly decreasing amplitudes. (For an excellent figure, reproduced from Jahnke & Emde (1943), see Cochran, Crick & Vand, 1952.) More precisely (Jahnke & Emde, 1943; Watson, 1944), for large p the first maximum of $J_p(x)$ is at $x \approx p + 0{\cdot}81^3\sqrt{p}$, while the oscillations for values of x larger than p are approximately described by the asymptotic expression

$$J_p(x) \sim (2/\pi x)^{\frac{1}{2}}[P_p(x) \cos (x - (2p+1)\pi/4) + Q_p(x) \sin (x - (2p+1)\pi/4)] , \tag{8}$$

where

$$P_p(x) = 1 - (4p^2-1)(4p^2-9)/2!(8x)^2 + \ldots ,$$
$$Q_p(x) = (4p^2-1)/8x + \ldots .$$

The dependence of the transform on the radial coordinate R is the following. For small values of R it is described by $J_0(2\pi rR)$, which starts at unity for $R = 0$ and oscillates about the R axis with an amplitude approximately given by $(\pi^2 rR)^{-\frac{1}{2}}$ and a distance between successive zeroes close to $\frac{1}{2}(1/r)$. Since a typical value of r is several hundred Å there will be several hundred oscillations for each Å^{-1} of R. When $2\pi rR$ reaches the value N, J_N and $J_{-N} = (-1)^N J_N$ start contributing, and more generally, each time $2\pi rR$ passes one of the values $nN(n = 1, 2, 3, \ldots)$ the pair of functions J_{nN} and J_{-nN} will begin to assume non-negligible values. All these functions have the same highly oscillatory nature as J_0 once they are past their first maximum, the oscillations being approximately of the same period $1/r$ in R and, eventually, of the same amplitude, $(\pi^2 rR)^{-\frac{1}{2}}$. The initial values of the amplitudes of the oscillation are rather larger than $(\pi^2 rR)^{-\frac{1}{2}}$ but less than $(2/\pi)^{\frac{1}{2}}(4\pi^2 r^2 R^2 - n^2 N^2)^{-\frac{1}{4}}$ (Watson, 1944). The high-order Bessel functions thus impart to the transform the characteristic feature that whenever $2\pi rR$ passes one of the values $nN(n = 1, 2, 3, \ldots)$ a band appears, with a sharp inside edge and an outside tail of slowly decreasing amplitude. In terms of R these edges occur whenever $R = nN/2\pi r = n/a$, which reflects the discrete nature of the circle, a being the distance between neighboring points. The rapid oscillations are a consequence of the large-scale features of the circle, and indeed the term $n = 0$ is the transform of a continuous circle:

$$T_{\text{cont.cir.}} = J_0(2\pi rR) . \tag{9}$$

With regard to the angular dependence of $T_{\text{cir.}}$ we note that the term $n = 0$ has circular symmetry. All other terms are of highly oscillatory nature, and have, individually, symmetry axes of the order $|n|N$.

Turning to the scattering intensity to be expected for the discrete circle, the square of the modulus of T shows rapid fluctuations of period $1/r$ in R and of periods $2\pi/(n-n')N$ in Φ. These fluctuations will scarcely be observable with the short-wavelength radiations required to analyze the fine structure of the object. Furthermore, usually not one but many circles or aggregates of such circles with different r, N, δ values will scatter at the same time, so that the fluctuations will be averaged out. To obtain a quantity characteristic of the observable scattering intensity we form the square of the modulus of T and average it over the rapid oscillations in R and in Φ.

The effect of averaging over Φ over a range of the order $2\pi/N$ is that all cross terms vanish, so that $\langle |T_{\text{cir.}}|^2 \rangle_{\text{av.}}$ has circular symmetry and contains only the squares of Bessel functions. Thus

$$\langle |T_{\text{cir.}}|^2 \rangle_{\text{av.}} \approx N^2[\langle J_0^2(2\pi rR) \rangle_{\text{av.}} + 2 \sum_{n=1}^{[aR]} \langle J_{nN}^2(2\pi rR) \rangle_{\text{av.}}] , \tag{10}$$

where $[aR]$ signifies the largest integer which is smaller than or equal to $2\pi rR/N = aR$. The averaging over the oscillations in R cannot be carried out exactly, but useful results will be obtained later on by employing the asymptotic expansion (8).

Consider next the transform of a set of points arranged at equal distances along a circular arc. It is essentially given by (6), except that j runs only to $(M-1)$, M being the total number of points. The sum over j is a geometrical series and results in a function closely related to the Laue function of crystallography. To simplify the phase constant, we choose the origin of the angular coordinates half-way along the arc, so that $\delta = -\pi(M-1)/N$ and obtain,

$$T_{\text{arc}}(R, \Phi) = M \sum_{p=-\infty}^{\infty} J_p(2\pi rR) \times \exp [ip(\Phi + \tfrac{1}{2}\pi)] \left[\frac{\sin (\pi pM/N)}{M \sin (\pi p/N)}\right] . \tag{11}$$

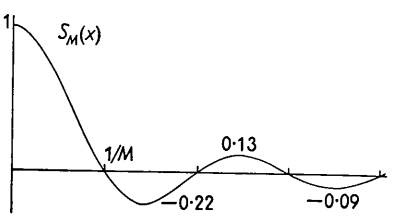

Fig. 1. The function $S_M(x)$ of equation (12), for $M \gg 1$ ($N \gg 1$).

The last factor is periodic in p with the period N, and attains its maximum value 1 whenever p is a multiple of N. Fig. 1 shows a graph of the related function $(p/N \rightarrow x)$

$$S_M(x) = M^{-1}(\sin \pi Mx)/\sin \pi x \qquad (12)$$

in the neighborhood of one of its maxima for which $x = n$, $p = nN$. (For the graph, M (and thus N) are assumed to be large.) The values of $S_M(p/N)$ decrease as the difference between $|p|$ and the nearest multiple of N increases. The first zero is reached when $|p-nN| = N/M$ so that the decrease of the factor is the more rapid the larger the angle subtended by the arc. Values of p for which $|p-nN| > N/M$ successively give rise to negative and positive contributions of ever decreasing magnitude. Thus for any sizeable fraction of the complete circle the transform contains essentially only Bessel functions whose order is in the neighborhood of multiples of N, the number of points that the *completed* discrete circle would contain.

The transform shows bands similar to those of the discrete circle. These bands occur again whenever R passes a multiple of $1/a$, but their edges are not quite as sharp as in the previous case, since the contributions to the nth band involve not only J_{nN} but also Bessel functions of neighboring orders.

The transform shows the same rapid oscillations in R of period $1/r$ discussed previously. In addition, the terms with p near $nN (n \neq 0)$ show rapid oscillations in Φ while those with p near 0 exhibit slow variation in the angular variable. Indeed, the low-order terms of T_{arc} represent the transform of a continuous arc of radius r, extending in angle from $-\Theta$ to $+\Theta$, where $\Theta = \pi M/N$,

$$\begin{aligned} T_{\text{cont. arc}}(R, \Phi) &= \sum_{p=-\infty}^{\infty} J_p(2\pi rR) \exp [ip(\Phi+\tfrac{1}{2}\pi)] (\sin p\Theta)/p\Theta \\ &= J_0(2\pi rR) + \sum_{p=1}^{\infty} i^p J_p(2\pi rR)[\sin p(\Phi+\Theta) \\ &\qquad -\sin p(\Phi-\Theta)]/p\Theta . \end{aligned} \qquad (13)$$

King & Lipscomb (1950) have given numerical values for the function

$$A(a, \theta) = \sum_{p=1}^{\infty} (2/p) i^p J_p(a) \sin p\theta$$

in terms of which the second sum above equals $[A(2\pi rR, \Phi+\Theta) - A(2\pi rR, \Phi-\Theta)]/2\Theta$.

To obtain a quantity representative of the observable intensity we average over the high-frequency oscillations in Φ and R. As a consequence no cross terms between the various groups of Bessel functions appear, and

$$\begin{aligned} \langle |T_{\text{arc}}(R, \Phi)|^2 \rangle_{\text{av.}} &\approx M^2 [\langle |T_{\text{cont. arc}}(R, \Phi)|^2 \rangle_{\text{av.}} \\ &+ 2 \sum_{n=1}^{[aR]} \langle | \sum_{p=-N/2}^{N/2} \exp ip(\Phi+\tfrac{1}{2}\pi) J_{nN+p}(2\pi rR) S_M(p/N)|^2 \rangle_{\text{av.}}]. \end{aligned} \qquad (14)$$

As in (10), the first term is representative of the large-scale structure, while the remaining sum accounts for the microscopic features of the object.

Transforms of cylinders

Consider a circular cylinder formed by suitably curving a rectangular net of points, one edge of the primitive unit cell, of length d, being parallel to the cylinder axis z, while the other has the approximate length a. This cylinder may be generated by replacing each point of a circular set by a perpendicular row of Q evenly spaced points having a repeat d. This operation is one of folding the set of Q row points with the circular point set (1) (see for instance Waser & Schomaker, 1953). The cylindrical coordinates of the resulting points are (r, φ_j, z_q), where

$$z_q = qd - (Q-1)d/2;\ q = 0, 1, 2, \ldots (Q-1) \qquad (15)$$

(choosing the z coordinates symmetrically relative to $z = 0$) and where the (r, φ_j) are identical with the plane polar coordinates discussed previously. The transform of this cylinder is defined by

$$T_{\text{rect.}} = \sum_{j=0}^{N-1} \sum_{q=0}^{Q-1} \exp 2\pi i(x_jX + y_jY + z_qZ) . \qquad (16)$$

The sums over j and q are independent of each other so that in terms of the cylindrical coordinates (R, Φ, Z) of Fourier space

$$\begin{aligned} &T_{\text{rect.}}(R, \Phi, Z) \\ &= T_{\text{cir.}}(R, \Phi) \exp [-\pi i(Q-1)dZ] \sum_{q=0}^{Q-1} \exp (2\pi iqdZ) \\ &= T_{\text{cir.}}(R, \Phi) \sin (Q\pi dZ)/\sin \pi dZ . \end{aligned} \qquad (17)$$

This is the *product* of the transforms of a circular point set with that of a row of Q evenly spaced points, in accordance with the folding operation just discussed. The second factor is the Laue function which is shown by Fig. 1, provided the scales of the coordinate axes are suitably modified and $Q \gg 1$. Its primary maxima occur whenever $Z = m/d$, $m = 0, \pm 1, \pm 2, \ldots$. They are of height Q and have widths of the order $1/Qd$ in Z. The transform is thus restricted to the neighborhood of planes $Z = m/d$, corresponding to the familiar layer lines. The dependence on (R, Φ) is the same for all values of Z and identical with that of the two-dimensional case. The intensity distribution associated with each layer is the one discussed for the discrete circle and the basic structure of the net is reflected by the location of the sharp edges of bands at $R = n/a$, $Z = m/d$. A central section through the transform containing the Z axis thus shows a structure reciprocal to that of the original net.

Another simple cylinder results from similarly curving a diamond-type net with a centered rectangular unit cell, so that the rectangle edge of length d is again parallel to the cylinder axis, the other edge being

of length a. This cylinder may be generated by the superposition of a cylinder of the type just discussed with an identical one, of the same axis, but displaced by a distance $d/2$ parallel to z and rotated through π/N (half the difference in angular coordinates of two adjacent points of the original circular set). The effect of the translation on the transform of the cylinder is multiplication by $\exp(2\pi i Zd/2)$, while rotation by π/N is taken into account by replacing the angle δ by $\delta+\pi/N$. The transform of the diamond cylinder is the sum of the transforms of these two cylinders, whence

$$T_{\text{diam.}}(R, \Phi, Z) = \frac{\sin Q\pi dZ}{\sin \pi dZ} \sum_{n=-\infty}^{\infty} J_{nN}(2\pi rR) \times \exp[inN(\Phi+\tfrac{1}{2}\pi-\delta)][1+\exp i\pi(-n+dZ)]. \quad (18)$$

If $Q \gg 1$ the Laue function is different from zero only in the immediate neighborhood of $Z = m/d$ so that the last factor in the above expression may be replaced by $(1+(-1)^{n+m})$, which vanishes unless $(n+m)$ is even. Thus, while the cross-section of each layer is described by 2 $(\sin Q\pi dZ)/\sin \pi dZ$, the dependence on (R, Φ) is the following:

Even layers $(Z = 2m/d)$:

$$N \sum_{n=-\infty}^{\infty} J_{2nN}(2\pi rR) \exp[i2nN(\Phi+\tfrac{1}{2}\pi-\delta)]. \quad (19)$$

Odd layers $(Z = (2m+1)/d)$:

$$N \sum_{n=-\infty}^{\infty} J_{(2n+1)N}(2\pi rR) \exp[i(2n+1)N(\Phi+\tfrac{1}{2}\pi-\delta)].$$

This transform shows again a band structure, and in a planar section containing the Z axis the edges of these bands lie near the nodes of a centered rectangular net. The edges of the rectangular unit cell of this net are of length $2/d$ parallel to Z and $2/a$ parallel to R, so that this net is again reciprocal to the original one. Note that only even layers contain the term $J_0(2\pi rR)$ characteristic of the continuous cylinder.

For the special cases that $d = a/\sqrt{3}$ and $d = \sqrt{3}.a$ the basic nets are hexagonal, one edge of the basic hexagon being parallel to the z axis in the first case and perpendicular in the second (Fig. 2).

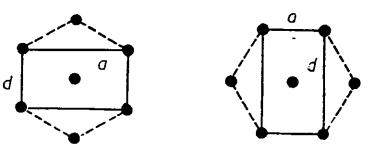

Fig. 2. Two orientations of a hexagonal net.

No detailed treatment will be given of the transforms of cylindrical fragments resulting from folding a row of points with points arranged along a circular arc. These transforms are related to those of discrete arcs in exactly the same way as discussed above for circular sets.

We discuss next the transform of a composite tube, made up of a number of concentric rectangular cylinders of the same length, formed of nets with the same unit cell. The radii of the various cylinders are to differ by multiples of a constant, t. Thus, if r_g is the radius of the gth cylinder and N_g the number of points along its circumference,

$$r_g = r+gt, \; 2\pi r_g \approx N_g a, \quad N_g \approx N+2\pi gt/a, \; g = 0, \pm1, \pm2, \ldots \pm G, \quad (20)$$

r and N being the averages of r_g and N_g. The number of cylinders is $K = 2G+1$. (The final result applies with appropriate meaning of the symbols to both odd and even K's.) We assign the angular constant δ_g to the gth cylinder and describe its position along the z axis by adding the constant ϱ_g to all z coordinates of (15). The transform reads

$$T_{K,\,\text{rect.}}(R, \Phi, Z) = \frac{\sin Q\pi dZ}{\sin \pi dZ} \sum_{g=-G}^{G} N_g \exp(2\pi i \varrho_g Z) \sum_{n=-\infty}^{\infty} J_{nN_g}(2\pi r_g R) \exp[inN_g(\Phi+\tfrac{1}{2}\pi-\delta_g)]. \quad (21)$$

We are interested again in the square of the modulus of this function, averaged over rapid oscillations in Φ and R. This averaging process necessitates assumptions regarding the values of the constants δ_g and ϱ_g. The angular constants δ_g of the different cylinders are presumably random in any actual case; even if two row lines of neighboring cylinders should be in exact juxtaposition, this phase relation will be lost for adjacent rows. However, several different assumptions regarding the translational constants ϱ_g are of interest. They are: (1) All ϱ_g have the same value, arbitrarily set equal to zero. (2) The ϱ_g are distributed randomly. (3) The ϱ_g depend linearly on g, $\varrho_g = g.\Delta$ ((1) is a special case of this). The physical implications of these three cases will be discussed later.

Forming the square of the modulus of (21) and averaging over rapid oscillations in Φ causes all cross terms between high-order Bessel functions associated with different values of n and between them and J_0 to vanish. Furthermore, owing to the randomness of the δ_g, cross terms involving different g's tend to vanish also, unless $n = 0$. Thus when $n \neq 0$ the characteristic bands described earlier appear again, having edges where $R = n/a(n = 1, 2, 3, \ldots)$. The structure of these bands is independent of the behavior of the ϱ_g. The nth band represents the sum of the squares of the Bessel functions of the orders $\pm nN_g$. As far as these bands are concerned, the intensities due to the component cylinders are additive.

There is, however, interference between the K terms containing $J_0(2\pi r_g R)$ $(n = 0)$. The details of this interference depend on the assumptions regarding ϱ_g and will now be discussed.

Case 1: *all* $\varrho_g = 0$

The sum of the K terms with $n = 0$ shows circular symmetry and is closely related to the transform of a tube consisting of $K = 2G+1$ continuous cylinders of length L,

$$T_{K,\text{cont.}}(R, Z) = \frac{\sin \pi LZ}{\pi Z} \sum_{g=-G}^{G} 2\pi r_g J_0(2\pi r_g R) . \quad (22)$$

(This transform has been normalized differently from (9) and (13). It does not show any layer structure.)

To investigate the behavior of the sum over the J_0 in (21) or (22) we employ the leading term of the asymptotic expansion (8). Thus

$$\Sigma_1 \equiv \sum_{g=-G}^{G} N_g J_0(2\pi r_g R) \sim (\pi^2 rR)^{-\frac{1}{2}} \sum_g (1-gt/2r) \times (N+2\pi gt/a) \cos [2\pi(r+gt)R-\pi/4] , \quad (23)$$

where terms in $(Gt/r)^2 \approx (W/D)^2$ have been neglected (W is the wall strength, D the average diameter of the tube). Expanding the cosine and summing over g, we obtain in the same approximation

$$\Sigma_1 \sim (\pi^2 rR)^{-\frac{1}{2}} NK [\cos (2\pi rR-\pi/4) \times S_K(tR) + \sin (2\pi rR-\pi/4)(W/2D) C_K(tR)] , \quad (24)$$

where

$$S_K(tR) = (\sin \pi KtR)/K \sin \pi tR$$

and

$$C_K(tR) = (K \cos \pi KtR \sin \pi tR - \cos \pi tR \sin \pi KtR)/K^2 \sin^2 \pi tR .$$

Fig. 1 represents S_K, while C_K is proportional to its derivative. We are interested in the square of (24), averaged over fluctuations of the period $1/r$ in R. The squares of the cosine and sine of argument $(2\pi rR-\pi/4)$ average to $\frac{1}{2}$, their product to zero, so that

$$\langle|\Sigma_1|^2\rangle_{\text{av.}} \sim (N^2K^2/2\pi^2 rR) \times [S_K^2(tR) + (W/2D)^2 C_K^2(tR)] . \quad (25)$$

The second term will be dropped since terms in $(W/D)^2$ have already been neglected and since C_K^2 is small compared to S_K^2 (see Fig. 3). If the higher terms of the asymptotic expansion (8) are included in (23) and terms in $(W/D)^2$ are neglected we find that the final result may be expressed in terms of J_0:

$$\langle|\Sigma_1|^2\rangle_{\text{av.}} \approx (NK)^2 \langle J_0^2(2\pi rR)\rangle_{\text{av.}} S_K^2(tR) . \quad (26)$$

Even for small values of R this expression seems to be better than is warranted by its derivation from an asymptotic expansion, as evidenced by more detailed analysis. (It tends, for instance, to the correct limit when R approaches zero.) Fig. 3 contains a graph of S_K^2 versus R (for $K \gg 1$). It is periodic in R with the period $1/t$. The main maxima occur when $R = j/t$ ($j = 0, 1, 2, \ldots$), are of height 1, and have a width of the order $1/Kt$. Expression (26) thus has a maximum of value $(NK)^2$ at $R = 0$, followed by much smaller subsidiary maxima of height $(t/2\pi^2 jr)(NK)^2$ at $R=j/t$. All layers have the same structure for this case.

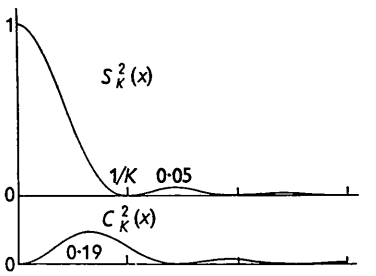

Fig. 3. The functions $S_K^2(x)$ and $C_K^2(x)$ defined by the expressions following equation (24), for $K \gg 1$.

Case 2: *random distribution of the* ϱ_g

The sum over all terms with $n = 0$ contains additional phase factors which all had unit value in (23),

$$\Sigma_2 \equiv \sum_g N_g J_0(2\pi r_g R) \exp (2\pi i \varrho_g Z) . \quad (27)$$

If the square of this sum is formed, the cross terms tend to vanish when $Z \neq 0$, owing to the randomness of the differences between the ϱ_g, and only the squares remain. However, when $Z = 0$ all phase factors have unit value and we obtain the previous result (26). Therefore,

$$\langle|\Sigma_2|^2\rangle_{\text{av.}} \approx \begin{cases} \sum_g N_g^2 \langle J_0^2(2\pi r_g R)\rangle_{\text{av.}}, & Z = m/d \neq 0 , \\ (NK)^2 \langle J_0^2(2\pi rR)\rangle_{\text{av.}} S_K^2(tR) , & Z = 0 . \end{cases} \quad (28)$$

The central portion of the equator has thus the same structure which all layers including the equator had in Case 1. For the central portions of the other layers there is in effect no coherence between the amplitudes due to the various component cylinders, and the intensities are additive. The maximum intensity of a layer (at $R = 0$) is proportional to K, the number of such cylinders, while it is proportional to K^2 for the equator.

Case 3: $\varrho_g = g.\Delta$

The sum over the terms $n = 0$ is now

$$\Sigma_3 \equiv \sum_g N_g J_0(2\pi r_g R) \exp (2\pi i g \Delta Z) . \quad (29)$$

A development for the mth layer ($Z = m/d$) similar to the one leading to (26) results in

$$\langle|\Sigma_3|^2\rangle_{\text{av.}} \approx (NK)^2 \langle J_0^2(2\pi rR)\rangle_{\text{av.}} \times [S_K(tR-m\Delta/d) + S_K(tR+m\Delta/d)]^2/4 . \quad (30)$$

There is thus a shift of the maxima of S_K^2 from $R = j/t$ in (23) to $R = j/t \pm m\Delta/dt$. Again the equator is identical with that for the previous two cases, while the mth layer shows the main maximum at $R = |m\Delta/dt|$ (provided $m|\Delta| < d/2$; otherwise the main

maximum will occur for the smallest value of $R = |j-m\Delta/d|/t)$. In any planar section through Fourier space containing the Z axis this maximum will of course show on both sides of the line $R = 0$.

Returning to the general discussion, we will briefly deal with the tube whose component cylinders are based on centered rather than primitive rectangular unit cells. The centered character of the unit cells will be reflected by the nature of the band structure of $\langle|T|^2\rangle_{\text{av.}}$, as discussed in the foregoing section (following equations (19)). Furthermore, for odd layers the central portion containing the J_0's will be absent so that the above remarks concerning the ϱ_g apply here to equator and even layers only.

Structure factors

The previous discussion has concerned itself entirely with sets of points each of which has to be replaced by the contents of a suitably oriented 'unit cell' for any actual case. Let the unit cell of a sheet, before being curved into a cylinder, contain H atoms with structure factors $f_h (h = 1, 2, \ldots, H)$. For simplicity we assume a rectangular set of axes, **x**, **y**, **z**, of lengths a, d, t. The parameters of atom h are u_h, v_h, w_h, and we assume that after the sheet has been curved, **y** points parallel to the z axis and **z** along the radial direction of the resulting cylinder (while **x** is perpendicular to both, Fig. 4). The coordinates of atom h in the 'unit cell' whose origin has the coordinates (r_g, φ_j, z_q) are given in Fig. 4.

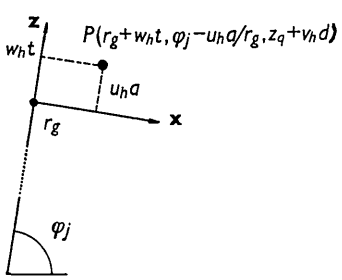

Fig. 4. Cylindrical coordinates of the center of atom h in 'unit cell' with origin at (r_g, φ_j, z_q).

The Fourier transform of the resulting aggregate of atoms is the sum of the H transforms of the point sets corresponding, severally, to the locations of all atoms h, each multiplied by the appropriate atomic scattering factor f_h. While for crystals, owing to the nature of lattices, it is possible to factor the complete transform into contributions representing the lattice type, the unit-cell contents, and the internal structure of the scattering atoms, no such exact factorization is possible in the present case. A similar separation does occur, however, in the approximation that the Bessel functions involved may be replaced by their asymptotic expansions.

A typical term in the complete transform is

$$\sum_{h=1}^{H} f_h \exp\left[2\pi i Z(z_q+v_h d)\right] J_{nN_g}[2\pi R(r_g+w_h t)] \times \exp\left[inN_g(\Phi+\tfrac{1}{2}\pi-\delta_g+u_h a/r_g)\right] . \quad (31)$$

It was shown previously that (in part owing to the randomness of the δ_g) $\langle|T|^2\rangle_{\text{av.}}$ does not contain cross terms between Bessel functions of different order, so that for $n \neq 0$ the square of the modulus of the above expression, averaged over rapid oscillations, represents the total contribution of this term to the intensity of a given band. The total intensity of this band will be given by the sum of all such contributions (31) which have the same value of $|n|$.

Accordingly, the leading term of the asymptotic expansion (8) is introduced into (31), followed by squaring and averaging. Neglecting terms in $w_h t/r$ and using $N_g a/r_g = 2\pi$ we obtain eventually

$$I_{nN_g} \sim (2\pi^2 r_g R)^{-1} \sum_h \sum_{h'} f_h f_{h'} \exp\left[2\pi i m(v_h-v_{h'})\right] \cos\left[2\pi Rt(w_h-w_{h'})\right] \exp\left[2\pi i n(u_h-u_{h'})\right] . \quad (32)$$

If higher terms of the expansion (8) are included in this development, the result can be recast in terms of J_{nN_g}. Furthermore, the double sum can be expressed as the sum of two squares, so that finally

$$I_{nN_g} \approx \langle J^2_{nN_g}(2\pi r_g R)\rangle_{\text{av.}} \tfrac{1}{2}\left[|F_{n,m}(R)|^2+|F_{n,m}(-R)|^2\right], \quad (33)$$

where

$$F_{n,m}(R) = \sum_{h=1}^{H} f_h \exp\left[2\pi i(nu_h+mv_h+Rtw_h\right] . \quad (34)$$

Note that $F_{n,m}(R)$ does not depend on the particular cylinder g whose contribution we are considering.

The terms $n = 0$ require separate treatment, as there may be interference among the amplitudes due to the different cylinders, depending on the behavior of the ϱ_g and the value of m. It turns out, however, that again the same factor as in (33) separates out and terms with $n = 0$ result in formulas analogous to (26), (28) and (30), but multiplied with $\frac{1}{2}(|F_{0,m}(R)|^2+|F_{0,m}(-R)|^2)$. All this is a consequence of our dealing, in the approximation chosen, essentially with exponential functions as is the case in the customary treatment of crystalline reflections. Our approximation is good only when $t \ll r$ and $a \ll r$, which implies small change in directions of the axes as one progresses from one 'unit cell' to the next along the circumference of the cylinder.

The complete expression for the intensity distribution in reciprocal space, caused by a composite tube consisting of K concentric cylinders, is thus

$$I(Z, R) \approx \frac{\sin^2 Q\pi dZ}{2\sin^2 \pi dZ}\Big\{\langle|\Sigma_i|^2\rangle_{\text{av.}}\left[|F_{0,m}(R)|^2+|F_{0,m}(-R)|^2\right]+\sum_{n=1}^{[aR]} N_g^2\langle J^2_{nN_g}(2\pi r_g R)\rangle_{\text{av.}}\left[|F_{n,m}(R)|^2+|F_{\bar{n},m}(R)|^2+|F_{n,m}(-R)|^2+|F_{\bar{n},m}(-R)|^2\right]\Big\}, \quad (35)$$

where $\langle|\Sigma_i|^2\rangle_{\text{av.}}$ is to be substituted from equations (26), (28) or (30) respectively, depending on which of the Cases 1–3 applies. The symbols N_g, r_g, Q, and $[aR]$ are defined by (20), (15) and the remark following (10), while the indices n and m characterize the edges of the bands situated at $R = n/a$, $Z = m/d$.

The intensity function (35) has radial symmetry, rapid fluctuations in Φ having been averaged over. The intensities of the various bands, as well as those of the central portions of the layers described by the functions J_0, are largely determined by the structure factors (34). We note that these factors (34) vary continuously with R so that the R-dependence of the various features is modified also. The effects of centering the unit cells of the original nets are, of course, contained implicitly in the structure factor and need no further discussion. (A particular case (the diamond net) has been dealt with earlier.)

The assumption of rectangular nets in a particular orientation is essential only for the exact form of (34) and not for the fact that a structure factor like (34) separates out. Nevertheless, even for more general types of 'unit cells' and their orientation relative to the cylinder it remains practical to describe the contents of each 'unit cell' in terms of rectangular coordinate axes oriented as above.

In summary, some important characteristics of the scattering of the tubular objects discussed are the following: The nature of the intensity function at small values of R is determined by the over-all structure of the tube, without much regard for its atomic make-up. The positions of the edges of the bands are characteristic of the type and the metric of the net underlying the structure, while the intensities of all features are largely determined by the contents of the 'unit cell'. Physical insight pertaining to the outside tails of the bands is obtained if it is remembered that any central planar *section* of a Fourier transform is determined by the *projection* of the contents of physical space on a plane parallel to this section (see for instance Waser & Schomaker, 1953). Thus, if the tube is projected on a plane containing the z axis the tails contained in the corresponding section through the transform are the result of the continually decreased spacings as one moves from the center line of the projection to its rims.

Discussion

The results of the foregoing sections find application to the following physical situations:

The scattering of a tube consisting of concentric cylinders with no interactions corresponds to Case 2 in which the ϱ_g are randomly distributed. If there is interaction among the component tubelets, Cases 1 or 3 may apply, or still other assumptions regarding the behavior of the ϱ_g may be made.

Cases 1 and 3 have, however, an important bearing on the problem of the scattering due to a wound-up sheet, as will now be discussed. For simplicity we will again use points rather than 'unit cells', the connection between the two now being clear.

Consider a rectangular net wound up along a planar spiral whose radius increases by t each time around, and let the net be so oriented that one of its principal axes remains parallel to the z direction. The resulting set of points has much in common with that of Case 1, where all $\varrho_g = 0$. Thus, a projection on a plane containing the z axis of a tube made of concentric cylinders with all ϱ_g equal will differ very little from a like projection of a sheet wound up in the fashion described. Since these projections determine the contents of appropriate sections through the corresponding transforms, these sections will show great similarity. To this extent the above discussion of Case 1 applies to the wound-up sheet. This correspondence holds to a lesser extent for sections inclined to the Z axis, the largest differences being expected for sections perpendicular to Z. While the intensity function for the composite tube has essentially circular symmetry, that for the wound-up sheet will contain terms dependent on Φ since the transition from one layer to the next occurs here in continuous dependence of φ. The correspondence between the two transforms will be the closer the smaller t/r.

If next a rectangular net is wound up on a slant, both of its sets of principal row lines are transformed into sets of spiral helices of slowly increasing radii (crossing each other at right angles). Considering the points along one of the helices of the set with the smaller pitch, we note a uniform increase of their z coordinates which is to some extent reflected by the behavior of the ϱ_g of Case 3. This correspondence is the closer, the smaller the pitch of the helix and the smaller t/r. The central portions of the layers of the transform of this coiled sheet will thus be approximated by those described for Case 3 with suitably changed spacing of the layers. However, winding the sheet on a slant has also twisted the orientation of the net so that the positions of the bands are affected. Viewing the tube perpendicularly to its axis, all portions of the net exactly in front of this axis will have suffered a twist by the angle of the slant, while all portions exactly in back will have suffered the opposite twist. Correspondingly, in any section through the transform containing the Z axis, there will now appear two edges for each edge of the case discussed in the foregoing. The location of these two edges may be obtained by rotating the section of the previous transform by plus or minus the angle of the slant. Sections not containing the Z axis will again show angular dependence, in contrast to corresponding sections through the transform of Case 3.

Analogous effects are expected for tubes made by winding up nets of lower than rectangular symmetry.

Finally, if a sheet consisting of more than one layer of unit cells is wound up, the scattering of the resulting tube shows features additional to those discussed. An important practical case is the one in which there is no interaction among the different layers of the sheet, correlations existing previous to the curving of the sheet being effectively destroyed by it. If there are I such layers, the essential traits of the scattering of such a coil are similar to those of a tube consisting of as many concentric tubelets as the coil has windings, each tubelet containing I evenly spaced simple cylinders with the following pattern of ϱ_g's. Let t_1 be the radius difference for adjacent cylinders within a tubelet, t_2 the distance between (say) the first cylinders of adjoining tubelets (t_2 need not be a multiple of t_1). The ϱ_g within a given tubelet have random values, while the ϱ_g of all cylinders separated by multiples of t_2 are related as in Case 1 or 3, depending on how the sheet is coiled. Accordingly, the intensity function behaves as discussed in the foregoing with the following changes and additional features. The distance t is replaced by t_2. Additional reflections appear on the equator, at $R = l/t_1$ ($l = 1, 2, 3, \ldots$). Owing to the randomness of the ϱ_g within a tubelet, no further reflections involving the reciprocal distance $1/t_1$ appear.

An example*

Fig. 5 shows (*a*) an electron-microscope picture of a halloysite tube about 40,000 Å long with an average thickness of about 700 Å; (*b*) its diffraction photograph with a wavelength of 0·038 Å (both reproductions by courtesy of Drs Taggart, Milligan & Studer (1954)). The diffraction pattern represents the intensity function on the surface of the (stationary) sphere of reflection oriented so that the Z axis is tangent to it. The picture thus approximately shows the contents of a planar section through reciprocal space containing the Z axis.

The pattern is in broad agreement with that expected for a hexagonal sheet with $d = a\sqrt{3} = 8{\cdot}78$ Å ($a = 5{\cdot}07$ Å) wound up on a slant of about $2\frac{1}{2}°$. Equatorial reflections occurring when Z is a multiple of 0·1445 Å^{-1} reveal that this sheet consists of layers of thickness $t_1 = 6{\cdot}92$ Å. The main maxima on the central portions of even layer lines (m even) may tentatively be interpreted to correspond to $\Delta' \approx 0{\cdot}8$ Å, where Δ' is the difference between Δ and the nearest multiple of d. Subsidiary maxima at distances of about 0·02 Å^{-1} from the corresponding main maxima then

* Modified 15 November 1954.

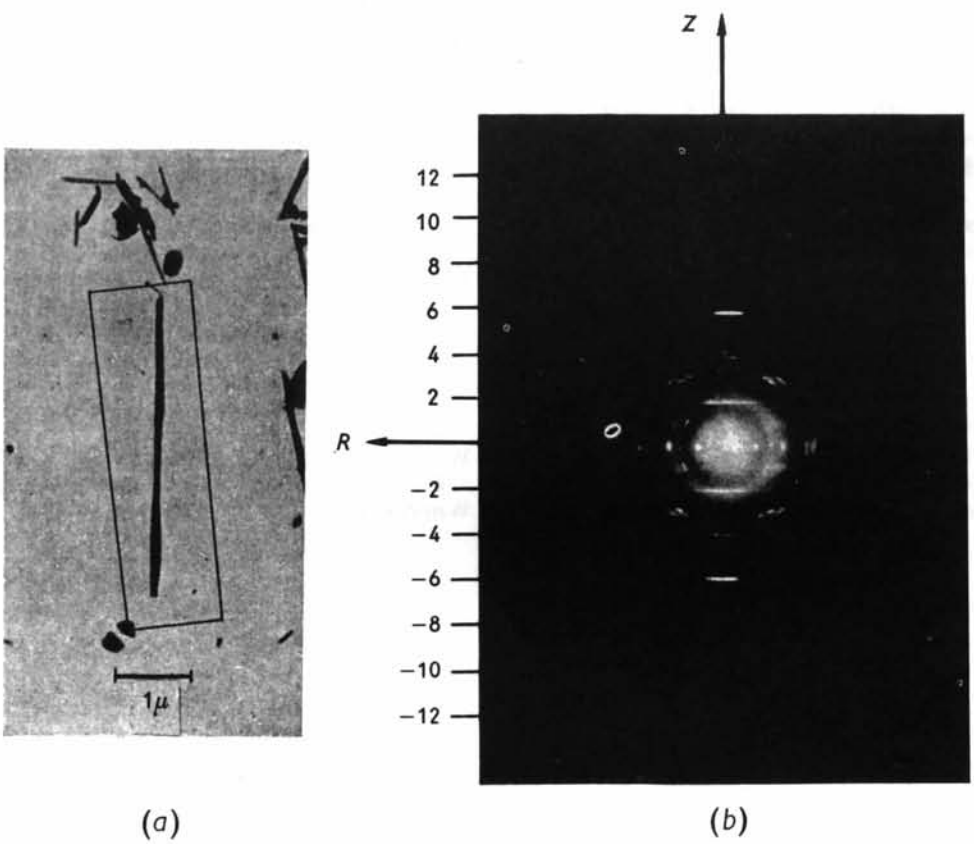

Fig. 5. (*a*) Electron-microscope picture of halloysite tube and (*b*) its scattering intensity (Taggart, Milligan & Studer, 1954). The numbers represent values of layer indices m. The black borders around the tube indicate the region used in the diffraction photograph.

indicate that the wound-up sheet has a thickness of the order of 50 Å, which is in accordance with the width of the 6·92 Å equatorial reflections. The apparent widths of the main maxima on even layer lines might suggest that there is little if any coherence from one winding to the next. This, however, would make it hard to understand the linear dependence on the layer index m of the distance from the Z axis of these maxima. Very likely Δ' is not constant and part of the broadening in the R direction is caused by its variation, so that the above value of 0·8 Å is an average only. Indeed, it appears from the electron-microscope picture of the object that the winding of the sheet is not completely regular.

Some weak reflections of the pattern reproduced in Fig. 5 are not accounted for. They may be caused by some fragments which are not part of the tube itself or may possibly be explained by a more exact theory of the scattering of a wound-up sheet which might also account for the fine structure of some of the bands. No attempt has been made to calculate the intensities of the various features in terms of the basic structure of the sheet.

Some of the fine structure of the bands may be interpreted in analogy to the mixed reflections expected for a rotating crystal in which the layers are arranged regularly. This is most apparent for the bands characterized by $n = 1$, $m = 3$ for which the analogues of $(hkl) = (130)$, (131) and (132) are present, where we have identified n with h and m with k, where l refers to the reciprocal-space coordinate perpendicular to the layers, and where the identity distance from layer to layer is $2t_1 = 13{\cdot}8$ Å.

This interpretation would imply that the layers making up a curved sheet have not become disordered through the curving. While order with respect to the z coordinate is not surprising, it is so with respect to the angular coordinate φ. To achieve it the unit cells of all layers along the circumference of the cylinder must match. Assuming an average radius of the tube of 350 Å and a thickness of the sheet of 50 Å, as much as 7% compression on the inside and 7% expansion on the outside are needed if the sheet is left intact. More likely would be the existence of a sufficient number of flaws or cracks to relieve part of the strain while the radial alignment is essentially maintained. Large enough fragments would have to be left intact to maintain a sufficient degree of coherence along the circumference.

Note added 15 *November* 1954.—Prof. P. P. Ewald has kindly sent me reprints of three papers by Jagodzinski & Kunze (1954*a*, *b*, *c*) and the proof of a paper by Whittaker (1954). Some of the results of the present paper are similar to results of these authors. Honjo & Mihama (1954) have very recently published electron-diffraction photographs of tubular halloysite specimens which they interpret by analogy with the case of a rotating single crystal.

I wish to thank Drs W. O. Milligan and H. P. Studer for bringing this problem to my attention, for comments regarding it, and for permission to use the photographs reproduced in Fig. 5; and Dr Gerald R. MacLane for a discussion regarding Bessel functions.

References

Cochran, W., Crick, F. H. C. & Vand, V. (1952). *Acta Cryst.* **5**, 581.

Honjo, G. & Mihama, K. (1954). *Acta Cryst.* **7**, 511.

Jagodzinski, H. & Kunze, G. (1954*a*). *Neues Jb. Miner. Mh.* p. 95.

Jagodzinski, H. & Kunze, G. (1954*b*). *Neues Jb. Miner. Mh.* p. 113.

Jagodzinski, H. & Kunze, G. (1954*c*). *Neues Jb. Miner. Mh.* p. 137.

Jahnke, E. & Emde, F. (1943). *Tables of Functions.* New York: Dover Publications.

King, M. V. & Lipscomb, W. N. (1950). *Acta Cryst.* **3**, 318.

Taggart, M. S., Milligan, W. O. & Studer, H. P. (1954). Third National Clay Minerals Conference, Houston, Texas, October 1954. To be published.

Waser, J. & Schomaker, V. (1953). *Rev. Mod. Phys.* **25**, 671.

Watson, G. N. (1944). *A Treatise on the Theory of Bessel Functions*, 2nd ed. Cambridge: University Press.

Whittaker, E. J. W. (1954). *Acta Cryst.* **7**, 827.